Exclusive processes $e^+e^- \to VP$ in k_T factorization

Cai-Dian Lü,[1,2] Wei Wang,[2,*] and Yu-Ming Wang[2,†]

[1]*CCAST (World Laboratory), P.O. Box 8730, Beijing 100080, People's Republic of China*

[2]*Institute of High Energy Physics, CAS, P.O. Box 918(4), 100049, People's Republic of China*

(Received 14 February 2007; published 24 May 2007)

The exclusive processes $e^+e^- \to VP$, in the region of which the final state meson momentum is much larger than the hadronic scale $\Lambda_{\rm QCD}$, are studied in the framework of the perturbative quantum chromodynamics (PQCD) approach based on the k_T factorization. Including the transverse momentum distribution in the light-cone wave functions, our results are consistent with the experimental measurements. According to our results, many processes have large enough cross sections to be detected at $\sqrt{s} =$ 10.58 GeV. The s dependence of the cross section has been directly studied and our result indicates that the $1/s^3$ scaling is more favored than $1/s^4$. We also find that the gluonic contribution for the processes involving $\eta^{(\prime)}$ is tiny.

DOI: 10.1103/PhysRevD.75.094020 PACS numbers: 13.66.Bc, 12.38.−t

I. INTRODUCTION

In exclusive or inclusive processes with large momentum transfers, the production rates and many other phenomena, such as the dimensional rule, the helicity structure, can be successfully explained by the perturbative QCD (PQCD) analysis [1,2]. The essential ingredient is the factorization theorem which ensures that a physical amplitude can be represented as a convolution of a hard scattering kernel and hadronic distribution amplitudes. The former can be calculated using the perturbation theory while the latter, although nonperturbative in nature, are universal. The light-cone distribution amplitudes which describe the longitudinal momentum distribution of partons in the hadron, can be determined by the experiments of various channels. In $e^+e^- \to \gamma^* \to VP$ at high energies (V denotes a light vector meson and P denotes a light pseudoscalar meson), the energy of the light meson is much larger than its mass and the hadronic scale $\Lambda_{\rm QCD}$. One important feature of this process is that the meson moves nearly on the light cone. The energetic light meson is composed of two valence quarks which are both energetic and collinear. The gluon which generates the quark pair is very hard and this leads to the application of perturbative QCD into this process. However, the application of the perturbative QCD approach to this simple process is complicated by the end point problem. If collinear factorization is applied, the hard kernel contains the inverse term of momentum fraction which makes the integration divergent at the end point. This divergence arises from the overlap of the soft and collinear momentum region.[1] A modified perturbative QCD approach based on k_T factorization, which keeps the intrinsic transverse momentum of partons in the meson, is proposed and successfully applied to many processes [4,5]. In this approach, the Sudakov effect is taken into account and the applicability of perturbative QCD can be extended down to a few GeV scale. It is claimed that the perturbative calculations could be consistent at scale about $Q \sim 20\Lambda_{\rm QCD}$ in this framework. This approach is also called the PQCD approach for simplicity.

The exclusive two-meson productions in e^+e^- annihilation provide an opportunity to investigate the behaviors of various meson form factors. The dependence of the form factor on the energy scale can shed light on the internal strong interaction information. It can also give information on the wave function of the hadron in terms of its partonic constituents. In the standard model, the exclusive production of hadron pairs at e^+e^- colliders can proceed through a virtual photon or a Z^0 boson. At energies well below the mass of Z^0, the production proceeds predominantly via the annihilation of e^+e^- into a virtual photon. Because of the invariance of charge conjugation in electromagnetic and strong interactions, the final state should have the same charge conjugation quantum number as a photon, i.e., these processes can only produce final states with charge conjugation quantum number $C = -1$. $e^+e^- \to VP$ can proceed via the following form factor:

$$\langle V(\epsilon, p_1)P(p_2)|j_\mu^{em}|0\rangle = F_{VP}(s)\epsilon_{\mu\nu\alpha\beta}\epsilon^\nu p_1^\alpha p_2^\beta, \qquad (1)$$

where $p_1(p_2)$ is the momentum of the vector (pseudoscalar) meson and ϵ is the polarization vector of the vector meson. Here j_μ^{em} is defined as $j_\mu^{em} = \bar{q}\gamma_\mu q$. Equation (1) indicates that the vector meson is transversely polarized. On the experimental side, the productions of VP have been extensively studied: BES and CLEO-c have reported the continuum productions [6–8]. Recently, the *BABAR* collaboration observed the exclusive reaction $e^+e^- \to \phi\eta$ at $\sqrt{s} = 10.58$ GeV and measured the cross section [9]. Since k_T factorization can give a reliable prediction in other similar processes, in this paper, we will perform a study

*Electronic address: wwang@mail.ihep.ac.cn

†Electronic address: wangym@mail.ihep.ac.cn

[1]This overlap has also been attempted to subtract out in Ref. [3] and new factorization theorems in rapidity space are subsequently achieved.

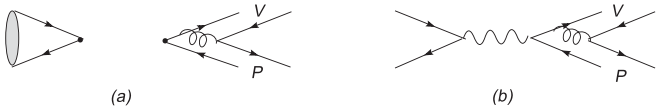

FIG. 1. The annihilation diagrams in B decays and e^+e^- annihilation. In the left diagram, the B meson is annihilated through the four-quark operator. In the right diagram, the electron and the positron annihilate into a virtual photon. These two diagrams have similar topologies.

on $e^+e^- \to \gamma^* \to VP$ in this framework and make a comparison with the data.

Another interesting reason for investigating the e^+e^- annihilation is the similarity with the annihilation corrections in B decays, shown in Fig. 1. In charmless two body B decays, the annihilation diagrams are power suppressed relative to the emission contribution. But it is found that in $B \to \pi K$, $\pi\pi$ decays, the factorizable annihilation diagrams could be important due to the chiral enhancement factor for operator O_6 [5]. This enhancement of factorizable diagrams can provide large strong phases and give large CP asymmetries, which indicates the annihilation diagrams are of great importance. Comparing the two diagrams in Fig. 1, we can see that the e^+e^- annihilations have similar topologies with the factorizable annihilation diagrams in B decays. They may provide an ideal laboratory to isolate the power correction effect and to find out whether contributions of annihilations from end point are important or not for meson productions [10].

The remainder of this paper is organized as follows. In Sec. II, we present the expression for the cross sections for $e^+e^- \to VP$ in the k_T factorization: the first part of this section is devoted to the discussion on the decay constants and the distribution amplitudes of mesons, and the second part is contributed to a brief introduction of the PQCD approach and factorization formulas for form factors. The numerical results and discussions are presented in Sec. III. The last section is our summary.

II. CALCULATION IN k_T FACTORIZATION

A. Decay constants and wave functions

The decay constants for a pseudoscalar meson and a vector meson are defined by

$$\begin{aligned}\langle P(P)|\bar{q}_2\gamma_\mu\gamma_5 q_1|0\rangle &= -if_P P_\mu,\\ \langle V(P,\epsilon)|\bar{q}_2\gamma_\mu q_1|0\rangle &= f_V m_V \epsilon_\mu,\\ \langle V(P,\epsilon)|\bar{q}_2\sigma_{\mu\nu} q_1|0\rangle &= -if_V^T(\epsilon_\mu P_\nu - \epsilon_\nu P_\mu),\end{aligned} \tag{2}$$

The pseudoscalar decay constants taken from the Particle Data Group [11] are shown in Table I. The charged vector meson longitudinal decay constants are extracted from the data on $\tau^- \to (\rho^-, K^{*-})\nu_\tau$, while the neutral vector meson longitudinal decay constants are determined from the data on the electromagnetic annihilation processes $V^0 \to e^+e^-$ [11]. The transverse decay constants are taken from the QCD sum rules [12,13], which are also collected in Table I.

TABLE I. Input values of the decay constants of the pseudoscalar and vector mesons (in MeV) [11–13].

f_π	f_K	f_ρ	f_ρ^T	f_ω	f_ω^T	f_{K^*}	$f_{K^*}^T$	f_ϕ	f_ϕ^T
131	160	209	165 ± 9	195	145 ± 10	217	185 ± 10	231	200 ± 10

The light-cone distribution amplitudes are defined by the matrix elements of the nonlocal operators at the lightlike separations z_μ with $z^2 = 0$, and sandwiched between the vacuum and the meson state. The two-particle light-cone distribution amplitudes of an outgoing pseudoscalar meson P, up to twist-3 accuracy, are defined by [14]

$$\begin{aligned}\langle P(P)|\bar{q}_{2\beta}(z)q_{1\alpha}(0)|0\rangle &= -\frac{i}{\sqrt{6}}\int_0^1 dx e^{ixP\cdot z}\Big[\gamma_5 \not{P}\phi^A(x)\\ &\quad + m_0\gamma_5\phi^P(x)\\ &\quad - m_0\sigma^{\mu\nu}\gamma_5 P_\mu z_\nu\frac{\phi^\sigma(x)}{6}\Big]_{\alpha\beta}\\ &= -\frac{i}{\sqrt{6}}\int_0^1 dx e^{ixP\cdot z}[\gamma_5\not{P}\phi^A(x)\\ &\quad + \gamma_5 m_0\phi^P(x)\\ &\quad + m_0\gamma_5(\not{n}\not{v} - 1)\phi^T(x)]_{\alpha\beta},\end{aligned} \tag{3}$$

where n, v are two light-cone vectors. The pseudoscalar meson is moving on the direction of n, with v the opposite direction. $m_0 = \frac{M_P^2}{m_{q_1}+m_{q_2}}$ is the chiral enhancement parameter. x is the momentum fraction carried by the positive quark q_2. We have performed the integration by parts for the third term and $\phi^T(x) = \frac{1}{6}\frac{d}{dx}\phi^\sigma(x)$. The explicit form of distribution amplitudes for pseudoscalar mesons have been studied in the QCD sum rule approach and other methods [15,16]. In principle, they are factorization scale dependent. Here we use the following form for leading-twist distribution amplitudes:

$$\phi_\pi^A(x) = \frac{3f_\pi}{\sqrt{6}}x(1-x)[1 + a_2^\pi C_2^{3/2}(t)], \tag{4}$$

$$\phi_K^A(x) = \frac{6f_K}{2\sqrt{6}}x(1-x)[1 + a_1^K C_1^{3/2}(t) + a_2^K C_2^{3/2}(t)], \tag{5}$$

where $t = 2x - 1$ and Gegenbauer polynomials are defined as

$$C_1^{3/2}(t) = 3t, \qquad C_2^{3/2}(t) = \tfrac{3}{2}(5t^2 - 1). \tag{6}$$

The Gegenbauer moments at $\mu = 1$ GeV are determined as

$$a_2^{\pi,K} = 0.25 \pm 0.15, \qquad a_1^K = 0.06 \pm 0.03. \tag{7}$$

Since the momentum transfer at $\sqrt{s} = 10.58$ GeV is large enough, the use of asymptotic forms for twist-3 distribu-

tion amplitudes is acceptable. Besides, we also use these forms at $\sqrt{s} = 3.67$ GeV for simplicity. The asymptotic forms of twist-3 distribution amplitudes are given by

$$\phi^P_{\pi(K)}(x) = \frac{f_{\pi(K)}}{2\sqrt{6}}, \qquad \phi^T_{\pi(K)}(x) = \frac{f_{\pi(K)}}{2\sqrt{6}}(1-2x). \quad (8)$$

As for the mixing of η and η', we use the quark flavor basis proposed by Feldmann and Kroll [17], i.e., these two mesons are made of $\bar{n}n = (\bar{u}u + \bar{d}d)/\sqrt{2}$ and $\bar{s}s$:

$$\begin{pmatrix} |\eta\rangle \\ |\eta'\rangle \end{pmatrix} = U(\theta)\begin{pmatrix} |\eta_n\rangle \\ |\eta_s\rangle \end{pmatrix}, \quad (9)$$

with the mixing matrix,

$$U(\theta) = \begin{pmatrix} \cos\theta & -\sin\theta \\ \sin\theta & \cos\theta \end{pmatrix}, \quad (10)$$

where the mixing angle $\theta = 39.3^\circ \pm 1.0^\circ$. In principle, this mixing mechanism is equivalent to the singlet and octet formalism, which is shown in [18]. But the advantage is transparent, since only two decay constants are needed:

$$\begin{aligned} \langle 0|\bar{n}\gamma^\mu\gamma_5 n|\eta_n(P)\rangle &= \frac{i}{\sqrt{2}} f_n P^\mu, \\ \langle 0|\bar{s}\gamma^\mu\gamma_5 s|\eta_s(P)\rangle &= i f_s P^\mu. \end{aligned} \quad (11)$$

We assume that the wave function of $\bar{n}n$ and $\bar{s}s$ is the same as the pion's wave function, except for the different decay constants and the chiral scale parameters:

$$f_n = (1.07 \pm 0.02) f_\pi, \qquad f_s = (1.34 \pm 0.06) f_\pi. \quad (12)$$

The chiral enhancement factors are chosen as

$$m_0^{\bar{n}n} = \frac{1}{2m_n}\left[m_\eta^2 \cos^2\theta + m_{\eta'}^2 \sin^2\theta - \frac{\sqrt{2} f_s}{f_n}(m_{\eta'}^2 - m_\eta^2)\cos\theta\sin\theta \right], \quad (13)$$

$$m_0^{\bar{s}s} = \frac{1}{2m_s}\left[m_{\eta'}^2 \cos^2\theta + m_\eta^2 \sin^2\theta - \frac{f_n}{\sqrt{2} f_s}(m_{\eta'}^2 - m_\eta^2)\cos\theta\sin\theta \right], \quad (14)$$

with $m_n = 5.6$ MeV and $m_s = 137$ MeV at $\mu = 1$ GeV [16].

In this work, we also investigate the gluonic contribution for isosinglet pseudoscalar meson η and η'. This contribution has been attempted in [18] with a negligible effect in the $B \to \eta$ form factor and a few percents to $B \to \eta'$. The leading-twist gluonic distribution amplitudes of the η_n and η_s mesons are defined as [19]

$$\begin{aligned} \langle \eta_n(P)|A^a_{[\mu}(z)A^b_{\nu]}(0)|0\rangle &= \frac{\sqrt{2} f_n}{\sqrt{3}} \frac{C_F}{4\sqrt{3}} \frac{\delta^{ab}}{N_c^2 - 1} \epsilon_{\mu\nu\rho\sigma} \frac{n_-^\rho P^\sigma}{n_- \cdot P} \times \int_0^1 dx e^{ixP\cdot z} \frac{\phi_n^G(x)}{x(1-x)}, \\ \langle \eta_s(P)|A^a_{[\mu}(z)A^b_{\nu]}(0)|0\rangle &= \frac{f_s}{\sqrt{3}} \frac{C_F}{4\sqrt{3}} \frac{\delta^{ab}}{N_c^2 - 1} \epsilon_{\mu\nu\rho\sigma} \frac{n_-^\rho P^\sigma}{n_- \cdot P} \times \int_0^1 dx e^{ixP\cdot z} \frac{\phi_s^G(x)}{x(1-x)}, \end{aligned} \quad (15)$$

where $A^a_{[\mu}(z)A^b_{\nu]}(w) \equiv [A^a_\mu(z)A^b_\nu(w) - A^a_\nu(z)A^b_\mu(w)]/2$ and the function [20],

$$\begin{aligned} \phi^G_{n(s)}(x) &= x^2(1-x)^2 B_2^{n(s)} C_1^{5/2}(2x-1), \\ C_1^{5/2}(t) &= 5t. \end{aligned} \quad (16)$$

The gluon labeled by the subscript μ carries the momentum fractions x based on the above definition. The two Gegenbauer coefficients B_2^n and B_2^s could not be the same in principle. However, it is acceptable to assume $B_2^n = B_2^s \equiv B_2$, since there are large uncertainties in their values. Here the range of B_2 has been extracted as $B_2 = 4.6 \pm 2.5$ [19].

Following the similar procedures as for the pseudoscalar mesons, we can derive the vector meson distribution amplitudes for the transverse polarization up to twist-3 [21]:

$$\langle V(P,\epsilon_T)|\bar{q}_{2\beta}(z)q_{1\alpha}(0)|0\rangle = \frac{1}{\sqrt{6}}\int_0^1 dx e^{ixP\cdot z}[M_V \not{\epsilon}_T \phi_V^v(x) + \not{\epsilon}_T \not{P} \phi_V^T(x) + M_V i\epsilon_{\mu\nu\rho\sigma}\gamma_5\gamma^\mu \times \epsilon_T^\nu n^\rho v^\sigma \phi_V^p(x)]_{\alpha\beta}, \quad (17)$$

where we have adopted the convention $\epsilon^{0123} = 1$ for the Levi-Civita tensor $\epsilon^{\mu\nu\alpha\beta}$.

The twist-2 distribution amplitudes for transversely polarized vector can be expanded as

$$\phi_\rho^T(x) = \frac{3 f_\rho^T}{\sqrt{6}} x(1-x)[1 + a_{2\rho}^\perp C_2^{3/2}(t)], \quad (18)$$

$$\phi_\omega^T(x) = \frac{3 f_\omega^T}{\sqrt{6}} x(1-x)[1 + a_{2\omega}^\perp C_2^{3/2}(t)], \quad (19)$$

$$\phi_{K^*}^T(x) = \frac{3 f_{K^*}^T}{\sqrt{6}} x(1-x)[1 + a_{1K^*}^\perp C_1^{3/2}(t) + a_{2K^*}^\perp C_2^{3/2}(t)], \quad (20)$$

$$\phi_\phi^T(x) = \frac{3 f_\phi^T}{\sqrt{6}} x(1-x)[1 + a_{2\phi}^\perp C_2^{3/2}(t)]. \quad (21)$$

The Gegenbauer moments have been studied extensively in the literature [21,22]; here we adopt the very recent updated form [12,13]:

$$a_{1K^*}^{\perp} = 0.04 \pm 0.03, \qquad a_{2\rho}^{\perp} = a_{2\omega}^{\perp} = 0.15 \pm 0.07,$$
$$a_{2K^*}^{\perp} = 0.11 \pm 0.09, \qquad a_{2\phi}^{\perp} = 0.06^{+0.09}_{-0.07}. \tag{22}$$

As for the twist-3 distribution amplitudes ϕ_V^p and ϕ_V^v, there are no recent updates associate with those updates for twist-2 distribution amplitudes [12,13], we also use the asymptotic form:

$$\phi_V^v(x) = \frac{3f_V}{8\sqrt{6}}[1 + (2x-1)^2],$$
$$\phi_V^p(x) = \frac{3f_V}{4\sqrt{6}}(1-2x). \tag{23}$$

The above discussions concentrated on the longitudinal momentum distribution and we intend to include the transverse momentum distribution functions of the pseudoscalar and vector mesons. But at present, the intrinsic transverse momentum dependence of wave function is still unknown from the first principle of QCD. As an illustration, we use a simple model in which the dependence of the wave function on the longitudinal and transverse momentum can be factorized into two parts [23]:

$$\psi(x, \mathbf{k}_T) = \phi(x) \times \Sigma(\mathbf{k}_T), \tag{24}$$

where $\phi(x)$ is the longitudinal momentum distribution amplitude discussed above and $\Sigma(\mathbf{k}_T)$ describes the transverse momentum distribution. $\Sigma(\mathbf{k}_T)$ satisfies the normalization conditions:

$$\int d^2\mathbf{k}_T \Sigma(\mathbf{k}_T) = 1. \tag{25}$$

In the following, we will use a Gaussian distribution:

$$\Sigma(\mathbf{k}_T) = \frac{\beta^2}{\pi} \exp(-\beta^2 \mathbf{k}_T^2), \tag{26}$$

where the parameter β characterizes the shape of the transverse momentum distribution. The numerical value for β can be fixed by the condition that the root mean square transverse momentum $\langle \mathbf{k}_T^2 \rangle^{1/2}$ should be at the order of $\Lambda_{\rm QCD}$. Their relation can be derived from

$$\langle \mathbf{k}_T^2 \rangle = \frac{\int_0^1 dx \int d^2\mathbf{k}_T \mathbf{k}_T^2 |\psi(x, \mathbf{k}_T)|^2}{\int_0^1 dx \int d^2\mathbf{k}_T |\psi(x, \mathbf{k}_T)|^2} = \frac{1}{2\beta^2}. \tag{27}$$

If we choose the root mean square transverse momentum $\langle \mathbf{k}_T^2 \rangle^{1/2} = 0.35$ GeV, then $\beta^2 = 4$ GeV^{-2}. In the PQCD approach, the integration will be transformed to the $\mathbf{b}$ space (coordinate space) and it is convenient to use the Fourier transformation of $\Sigma(\mathbf{k}_T)$:

$$\Sigma(\mathbf{b}) = \int d^2\mathbf{k}_T e^{-i\mathbf{k}_T \cdot \mathbf{b}} \Sigma(\mathbf{k}_T) = \exp\left(-\frac{b^2}{4\beta^2}\right). \tag{28}$$

It can be observed that, in the limit $\beta \to \infty$, $\Sigma(\mathbf{b})$ can be simply replaced by 1.

B. Form factor and cross section in k_T factorization

In the center of mass frame, we define q_1, q_2, p_1, and p_2 to be the four-momenta of e^+, e^- in initial states, vector (V) and pseudoscalar meson (P) in final states, and define $k_{1(2)}$ and $x_{1(2)}$ to be the momenta and momentum fractions of the positive quarks inside V and P, respectively. The center mass energy of this process is denoted by $Q = \sqrt{s}$. Using the definition of the form factor in Eq. (1), we can obtain the cross section as

$$\sigma(e^+e^- \to VP) = \frac{\pi\alpha_{em}^2}{6} |F_{VP}|^2 \Phi^{3/2}(s), \tag{29}$$

with

$$\Phi(s) = \left[1 - \frac{(m_V + m_P)^2}{s}\right]\left[1 - \frac{(m_V - m_P)^2}{s}\right]. \tag{30}$$

There are four different types of diagrams contributing to the productions of vector and pseudoscalar mesons in e^+e^- annihilations, to the leading order of the strong and electromagnetic coupling constants. The first type of diagrams contributing to this process is displayed in Fig. 2. These diagrams give the dominant contribution. The diagrams in Fig. 3 contribute to the processes involving η and η', while the diagrams in Fig. 4 only contribute to the processes involving the neutral vector mesons ρ^0, ω, and ϕ. Although these diagrams are suppressed by α_{em}, they can be enhanced by $s/\Lambda_{\rm QCD}^2$. This mechanism is similar to the enhancement in penguin-dominated B decays [24] and the so-called fragmentation mechanism in $e^+e^- \to VV$ processes [25]. It is also interesting to explore this effect in $e^+e^- \to VP$. For $e^+e^- \to K^*K$ and $e^+e^- \to \rho^+\pi^-$, the two photon nonfragmentation diagrams can give their contributions as in Fig. 5. But these diagrams suffer the suppression from electromagnetic coupling constant α_{em} which can be neglected safely.

We begin with a brief review of the PQCD approach. The basic idea of the PQCD approach is that it takes into account the transverse momentum of valence quarks which results in the Sudakov factor. The form factor, taking the first diagram in Fig. 2 as an example, can be expressed as the convolution of the wave functions ψ_V, ψ_P and the hard scattering kernel T_H by both the longitudinal and the transverse momenta:

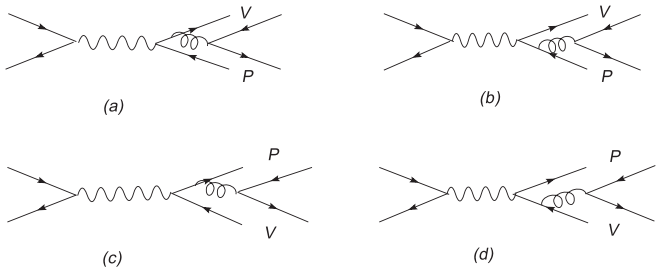

FIG. 2. Dominant contribution of $e^+e^- \to VP$.

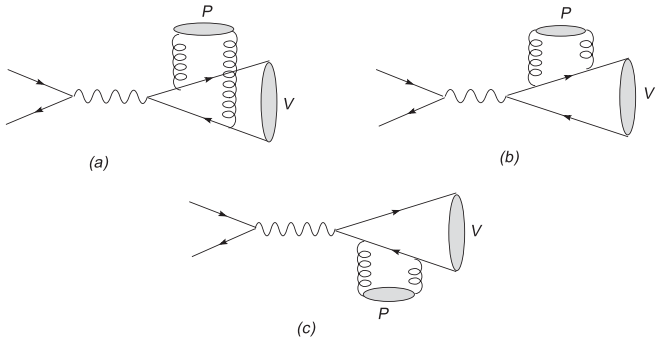

FIG. 3. Gluonic contributions.

$$F_a(VP) = \int_0^1 dx_1 dx_2 \int d^2\mathbf{k}_{T_1} d^2\mathbf{k}_{T_2} \psi_V(x_1, \mathbf{k}_{T_1}, p_1, \mu) \times T_H(x_1, x_2, Q, \mathbf{k}_{T_1}, \mathbf{k}_{T_2}, \mu)\psi_P(x_2, \mathbf{k}_{T_2}, p_2, \mu). \tag{31}$$

Through the Fourier transformation, the above equation can be expressed as

$$F_a(s) = \int_0^1 dx_1 dx_2 \int \frac{d^2\mathbf{b}_1}{(2\pi)^2} \frac{d^2\mathbf{b}_2}{(2\pi)^2} \mathcal{P}_V(x_1, \mathbf{b}_1, p_1, \mu) \times T_H(x_1, x_2, Q, \mathbf{b}_1, \mathbf{b}_2, \mu)\mathcal{P}_P(x_2, \mathbf{b}_2, p_2, \mu). \tag{32}$$

Here $\mathcal{P}_i(x_j, \mathbf{b}_j, p_j, \mu)$ are the Fourier transformation of $\psi_i(x_j, \mathbf{k}_{T_j}, p_j, \mu)$, where the subscript i denotes V or P, and j indicates 1 or 2.

In the above expression, the double logarithms, arising from the overlap of the soft and collinear divergence, have been resummed to result in the Sudakov factor [26]

$$\mathcal{P}_i(x_j, \mathbf{b}_j, p_j, \mu) = \exp[-s(x_j, b_j, Q) - s(1 - x_j, b_j, Q)]\tilde{\mathcal{P}}_i(x_j, \mathbf{b}_j, \mu). \tag{33}$$

The exponent $s(\xi, b_j, Q)$, $\xi = x_j$, or $1 - x_j$, is expressed as

$$s(\xi, b_j, Q) = \int_{1/b_j}^{\xi Q/\sqrt{2}} \frac{dp}{p}\left[\ln\left(\frac{\xi Q}{\sqrt{2}p}\right)A(\alpha_s(p)) + B(\alpha_s(p))\right], \tag{34}$$

where the anomalous dimensions A and B to one loop are given by

$$A = C_F\frac{\alpha_s}{\pi}, \qquad B = \frac{2}{3}\frac{\alpha_s}{\pi}\ln\left(\frac{e^{2\gamma_E - 1}}{2}\right), \tag{35}$$

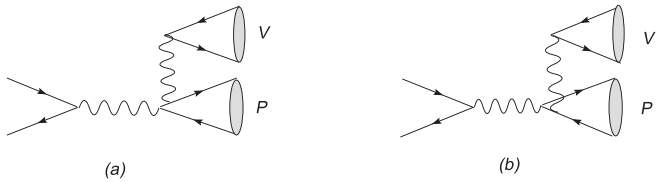

FIG. 4. Enhanced diagrams for the neutral vector mesons ρ^0, ω, and ϕ production.

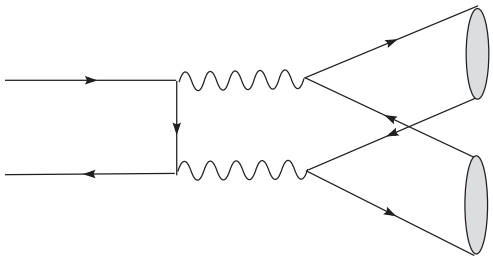

FIG. 5. Two photon nonfragmentation diagram. This contribution is suppressed by α_{em} and can be neglected.

with $C_F = \frac{N_c^2 - 1}{2N_c}$ and γ_E being the Euler constant. The one-loop running coupling constant,

$$\frac{\alpha_s(\mu)}{\pi} = \frac{4}{\beta_0 \ln(\mu^2/\Lambda^2_{\rm QCD})}, \tag{36}$$

with the coefficient

$$\beta_0 = \frac{33 - 2n_f}{3}, \tag{37}$$

where n_f is the number of the active quark number. We require the relation of the involved scales $\xi Q/\sqrt{2} > 1/b_j > \Lambda$ as indicated by the bounds of the variable p in Eq. (34). The QCD dynamics below $1/b_j$ scale is regarded as being nonperturbative which can be absorbed into the initial condition $\tilde{\mathcal{P}}_i(x_j, \mathbf{b}_j, \mu)$.

The form factor, as a physical observable, is independent of renormalization scale μ, but the functions $\tilde{\mathcal{P}}$ and T_H still contain single logarithms from ultraviolet divergences, which can be summed using the renormalization group equation method. This renormalization group analysis applied to T_H gives

$$T_H(x_j, \mathbf{b}_j, Q, \mu) = \exp\left[-4\int_\mu^t \frac{d\bar{\mu}}{\bar{\mu}}\gamma_q(\alpha_s(\bar{\mu}))\right] \times T_H(x_j, \mathbf{b}_j, Q, t), \tag{38}$$

where $\gamma_q = -\alpha_s/\pi$ is the quark anomalous dimension in the axial gauge and t is the largest mass scale involved in the hard scattering,

$$t = \max(\sqrt{x_2}Q, 1/b_1, b_2). \tag{39}$$

The scale $\sqrt{x_2}Q$ is associated with the longitudinal momentum of the quark propagator and $1/b_j$ is relate to the transverse momentum. The large-b_j behavior of $\mathcal{P}$ is summarized as

$$\mathcal{P}_i(x_j, \mathbf{b}_j, p_j, \mu) = \exp\left[-s(x_j, b_j, Q) - s(1 - x_j, b_j, Q) - 2\int_{1/b_j}^{\mu} \frac{d\bar{\mu}}{\bar{\mu}}\gamma_q(\alpha_s(\bar{\mu}))\right] \times \tilde{\mathcal{P}}_i(x, \mathbf{b}_j, 1/b_j), \tag{40}$$

where $\bar{\mathcal{P}}_i(x_j, \mathbf{b}_j, 1/b_j)$ is the wave function discussed above:

$$\bar{\mathcal{P}}_i(x_j, \mathbf{b}_j, 1/b_j) = \phi(x_j, 1/b_j) \times \Sigma(\mathbf{b}_j). \tag{41}$$

The threshold resummation [27,28] can also play an important role in $e^+e^- \to VP$ processes. The lowest-order diagrams [Figs. 2(a) and 2(d)] give an amplitude proportional to $1/(x_2^2(1-x_1))$ and $1/(x_2^2 x_1)$, respectively. In the threshold region with $x_2 \to 0$ [to be precise, $x_2 \sim O(\Lambda^2_{\rm QCD}/s)$], additional collinear divergences are associated with the internal quark. The QCD loop correction to the electromagnetic vertex can produce the double logarithm $\alpha_s \ln^2 x_2$ and resummation of this type of double logarithms leads to the Sudakov factor $S_t(x_2)$. Similarly, resummation of $\alpha_s \ln^2 x_1$ due to loop corrections in the other diagrams lead to the Sudakov factor $S_t(x_1)$. The Sudakov factor from threshold resummation is universal, independent of flavors of internal quarks, twists, and the specific processes. To simplify the analysis, the following parametrization has been used [28]:

$$S_t(x) = \frac{2^{1+2c}\Gamma(3/2+c)}{\sqrt{\pi}\Gamma(1+c)}[x(1-x)]^c, \tag{42}$$

with the parameter $c = 0.3$. This parametrization, symmetric under the interchange of x and $1-x$, is convenient for evaluation of the amplitudes. It is obvious that the threshold resummation modifies the end point behavior of the meson distribution amplitudes, rendering them vanish faster at $x \to 0$.

Combing all the above ingredients, we obtain the factorization formula for the contribution from Fig. 2(a):

$$\begin{aligned} F_a(VP) = {} & 16\pi C_F Q r_1 \int_0^1 dx_1 dx_2 \int_0^\infty b_1 db_1 b_2 db_2 \\ & \times \phi_P^A(x_2, b_2)[\phi_V^p(x_1, b_1) \\ & - \phi_V^v(x_1, b_1)]E(t_a)h(1-x_1, x_2, b_1, b_2), \end{aligned} \tag{43}$$

where h and E are defined by [5]

$$\begin{aligned} h(x_1, x_2, b_1, b_2) = {} & \left(\frac{i\pi}{2}\right)^2 S_t(x_2)[\theta(b_1-b_2)H_0^{(1)}(\sqrt{x_2}Qb_1) \\ & \times J_0(\sqrt{x_2}Qb_2) + \theta(b_2-b_1)H_0^{(1)}(\sqrt{x_2}Qb_2) \\ & \times J_0(\sqrt{x_2}Qb_1)]H_0^{(1)}(\sqrt{x_1 x_2}Qb_1), \end{aligned} \tag{44}$$

$$E(t_a) = \alpha_s(t_a)\exp[-S_1(t_a) - S_2(t_a)], \tag{45}$$

where J_0 and $H_0^{(1)}$ are the Bessel functions, respectively, $t_a = \max(\sqrt{x_2}Q, 1/b_1, 1/b_2)$ and $r_1 = M_V/Q$.

Similarly, for the other diagrams, the amplitudes are

$$\begin{aligned} F_b(VP) = {} & -16\pi C_F Q \int_0^1 dx_1 dx_2 \int_0^\infty b_1 db_1 b_2 db_2 \\ & \times E(t_b)h(x_2, 1-x_1, b_2, b_1) \times \{r_1(x_1-1) \\ & \times [\phi_1^p(x_1, b_1) + \phi_1^v(x_1, b_1)]\phi_2^A(x_2, b_2) \\ & + 2r_2\phi_1^T(x_1, b_1)\phi_2^p(x_2, b_2)\}, \end{aligned} \tag{46}$$

$$\begin{aligned} F_c(VP) = {} & -16\pi C_F Q \int_0^1 dx_1 dx_2 \int_0^\infty b_1 db_1 b_2 db_2 \\ & \times E(t_c)h(1-x_2, x_1, b_2, b_1) \times [r_1 x_1(\phi_1^p(x_1, b_1) \\ & - \phi_1^v(x_1, b_1))\phi_2^A(x_2, b_2) \\ & + 2r_2\phi_1^T(x_1, b_1)\phi_2^p(x_2, b_2)], \end{aligned} \tag{47}$$

$$\begin{aligned} F_d(VP) = {} & -16\pi C_F Q r_1 \int_0^1 dx_1 dx_2 \int_0^\infty b_1 db_1 b_2 db_2 \\ & \times E(t_d)h(x_1, 1-x_2, b_1, b_2) \times (\phi_1^p(x_1) \\ & + \phi_1^v(x_1))\phi_2^A(x_2, b_2), \end{aligned} \tag{48}$$

with $r_2 = m_0/Q$. The factorization scales t_i are chosen as

$$\begin{aligned} t_b &= \max(\sqrt{1-x_1}Q, 1/b_1, 1/b_2), \\ t_c &= \max(\sqrt{x_1}Q, 1/b_1, 1/b_2), \\ t_d &= \max(\sqrt{1-x_2}Q, 1/b_1, 1/b_2). \end{aligned} \tag{49}$$

If the final state meson is not K^* or K, the distribution amplitudes are completely symmetric or antisymmetric under the interchange of x_j and $1-x_j$. Then one can easily obtain

$$F_a(VP) = F_d(VP), \qquad F_b(VP) = F_c(VP). \tag{50}$$

For the flavor-singlet pseudoscalar meson η and η', there are additional contributions from the two-gluon diagrams as displayed in Fig. 3, even if they may be suppressed by the gluonic distribution amplitudes. However, it is still worthwhile to investigate the numerical contribution in order to make our calculations as complete as possible. The computations of these diagrams are similar to those shown in Fig. 2. The explicit calculations show that Fig. 3(a) does not contribute to the transition amplitude, due to the antisymmetry of the two gluons. The amplitudes of the other two diagrams are given by

$$\begin{aligned} F_e(V\eta_s) = {} & -8\pi Q r_1 \frac{f_s C_F^2\sqrt{2N_c}}{3(N_c^2-1)} \int_0^1 dx_1 dx_2 \\ & \times \int_0^\infty b_1 db_1 b_2 db_2 E(t_e)h(x_2, x_1, b_1, b_2) \\ & \times [(x_2+1)\phi_V^v(x_1, b_1) - (x_2-1)\phi_V^p(x_1, b_1)] \\ & \times \frac{\phi_s^G(x_2, b_2)}{x_2(1-x_2)}, \end{aligned} \tag{51}$$

$$F_f(V\eta_s) = 8\pi Q r_1 \frac{f_s C_F^2 \sqrt{2N_c}}{3(N_c^2-1)} \int_0^1 dx_1 dx_2 \times \int_0^\infty b_1 db_1 b_2 db_2 E(t_f) h(1-x_2, 1-x_1, b_1, b_2) \times (x_1-1)[(x_2-2)\phi_V^v(x_1,b_1) - x_2\phi_V^p(x_1,b_1)] \times \frac{\phi_s^G(x_2,b_2)}{x_2(1-x_2)}, \quad (52)$$

for $e^+e^- \to V\eta_s$ process with

$$t_e = \max(\sqrt{x_1}Q, 1/b_1, 1/b_2), \quad t_f = \max(\sqrt{1-x_1}Q, 1/b_1, 1/b_2). \quad (53)$$

It should be pointed out that the factor "2" from the exchange of two identical gluons in the final states has been added in the above equations. The amplitude for $e^+e^- \to V\eta_n$ can be easily obtained by replacing the corresponding decay constant with an additional factor $\sqrt{2}$ from Eqs. (51) and (52).

Furthermore, there are also contributions from the transition of photon radiated from one valence quark in pseudoscalar meson into a vector meson directly, which have been presented in Fig. 4. Although these diagrams may be suppressed by the coupling constant of electromagnetic interactions, they are also enhanced by the almost on-shell photon propagator compared with the first type diagrams, especially for the processes with a very large center mass energy. These diagrams can also be calculated according to k_T factorization; however, we will simply adopt collinear factorization due to disappearance of infrared divergence for these two diagrams. These two amplitudes are equal after integrating the momentum fractions carried by the valence quark of the meson. Hence, we obtain the amplitudes corresponding to them as follows:

$$F_g(VP) = F_h(VP) = \frac{12\pi\alpha_{em} f_V f_P}{M_V s}(1 + a_2^p). \quad (54)$$

The form factors for the explicit channels can be easily obtained from the combinations of the eight amplitudes F_{a-h}. To be more specific, we can write them as

$$F_{\rho^+\pi^-} = \tfrac{1}{3}[F_a(\rho\pi) + F_b(\rho\pi)], \quad (55)$$

$$F_{\rho^0\pi^0} = \tfrac{1}{3}[F_a(\rho\pi) + F_b(\rho\pi)] + \tfrac{1}{6}[F_g(\rho\pi) + F_h(\rho\pi)], \quad (56)$$

$$F_{\omega\pi^0} = [F_a(\omega\pi) + F_b(\omega\pi)] + \frac{1}{18}[F_g(\rho\pi) + F_h(\rho\pi)], \quad (57)$$

$$F_{\phi\pi^0} = -\frac{\sqrt{2}}{18}[F_g(\phi\pi) + F_h(\phi\pi)], \quad (58)$$

$$F_{K^{*+}K^-} = \tfrac{2}{3}[F_a(K^*K) + F_b(K^*K)] - \tfrac{1}{3}[F_c(K^*K) + F_d(K^*K)], \quad (59)$$

$$F_{K^{*0}\bar{K}^0} = -\tfrac{1}{3}[F_a(K^*K) + F_b(K^*K)] - \tfrac{1}{3}[F_c(K^*K) + F_d(K^*K)]. \quad (60)$$

The form factor of $e^+e^- \to \rho\eta^{(\prime)}$ can be written as the combination of its $\bar{n}n$ and $\bar{s}s$ component:

$$F_{V\eta} = \cos\theta F_{V\eta_n} - \sin\theta F_{V\eta_s}, \quad (61)$$

$$F_{V\eta'} = \sin\theta F_{V\eta_n} + \cos\theta F_{V\eta_s}, \quad (62)$$

where $V = \rho^0, \omega, \phi$ and

$$F_{\rho^0\eta_n} = [F_a(\rho\eta_n) + F_b(\rho\eta_n)] + \frac{1}{\sqrt{2}}[F_e(\rho\eta_n) + F_f(\rho\eta_n)] + \frac{5}{18}[F_g(\rho\eta_n) + F_h(\rho\eta_n)], \quad (63)$$

$$F_{\rho^0\eta_s} = \frac{1}{\sqrt{2}}[F_e(\rho\eta_s) + F_f(\rho\eta_s)] - \frac{\sqrt{2}}{6}[F_g(\rho\eta_s) + F_h(\rho\eta_s)], \quad (64)$$

$$F_{\omega\eta_n} = \frac{1}{3}[F_a(\omega\eta_n) + F_b(\omega\eta_n)] + \frac{\sqrt{2}}{6}[F_e(\omega\eta_n) + F_f(\omega\eta_n)] + \frac{5}{54}[F_g(\omega\eta_n) + F_h(\omega\eta_n)], \quad (65)$$

$$F_{\omega\eta_s} = \frac{\sqrt{2}}{6}[F_e(\omega\eta_s) + F_f(\omega\eta_s)] - \frac{\sqrt{2}}{18}[F_g(\omega\eta_s) + F_h(\omega\eta_s)], \quad (66)$$

$$F_{\phi\eta_n} = -\frac{1}{3}[F_e(\phi\eta_n) + F_f(\phi\eta_n)] - \frac{5\sqrt{2}}{54}[F_g(\phi\eta_n) + F_h(\phi\eta_n)], \quad (67)$$

$$F_{\phi\eta_s} = -\frac{2}{3}[F_a(\phi\eta_s) + F_b(\phi\eta_s)] - \frac{1}{3}[F_e(\phi\eta_s) + F_f(\phi\eta_s)] - \frac{1}{27}[F_g(\phi\eta_s) + F_h(\phi\eta_s)]. \quad (68)$$

III. NUMERICAL RESULTS AND DISCUSSIONS

A. Cross section

Making use of the distribution amplitudes and the inputs listed before, one can easily obtain the cross sections for the process $e^+e^- \to PV$. Here we would like to present the results of cross sections at $\sqrt{s} = 3.67$ GeV and 10.58 GeV in Table II together with the data measured by CLEO-c and the *BABAR* collaboration. The different scenarios $S1$, $S2$, $S3$ denoting different transverse momentum distribution functions, which will be discussed in the next subsection. As the longitudinal decay constants of the vector mesons and the pseudoscalar meson decay constants are precisely determined, the uncertainties from these inputs are neglected. Therefore the uncertainties shown in Table II are from the transverse decay constants of the vector meson given in Table I.

TABLE II. Results of $e^+e^- \to VP$ cross sections at $\sqrt{s} = 3.67$ GeV and $\sqrt{s} = 10.58$ GeV using three different transverse momentum distribution functions, denoted as $S1$, $S2$, and $S3$, respectively. The experimental results from the CLEO-c and *BABAR* collaborations are also included.

Channel	$\sqrt{s} = 3.67$ GeV				$\sqrt{s} = 10.58$ GeV			
	σ_{S1} (pb)	σ_{S2} (pb)	σ_{S3} (pb)	$\sigma_{\rm exp}$ (pb)	σ_{S1} (fb)	σ_{S2} (fb)	σ_{S3} (fb)	$\sigma_{\rm exp}$ (fb)
$\rho^+\pi^-$	$3.8^{+0.3}_{-0.2}$	$1.9^{+0.1}_{-0.2}$	$2.9^{+0.2}_{-0.2}$	$4.8^{+1.5+0.5}_{-1.2-0.5}$	$0.71^{+0.04}_{-0.04}$	$0.55^{+0.03}_{-0.03}$	$0.68^{+0.04}_{-0.04}$	
$\rho^0\pi^0$	$3.8^{+0.3}_{-0.2}$	$1.9^{+0.1}_{-0.2}$	$2.9^{+0.2}_{-0.2}$	$3.1^{+1.0+0.4}_{-0.8-0.4}$	$0.64^{+0.04}_{-0.04}$	$0.50^{+0.04}_{-0.03}$	$0.62^{+0.04}_{-0.03}$	
$\omega\pi^0$	$28.2^{+2.2}_{-2.2}$	$13.8^{+1.1}_{-1.1}$	$21.2^{+1.7}_{-1.6}$	$15.2^{+2.8+1.5}_{-2.4-1.5}$	$5.2^{+0.4}_{-0.3}$	$4.1^{+0.5}_{-0.3}$	$5.0^{+0.4}_{-0.3}$	
$\phi\pi^0$	1.2×10^{-4}	1.2×10^{-4}	1.2×10^{-4}	<2.2	2.1×10^{-3}	2.1×10^{-3}	2.1×10^{-3}	
$K^{*+}K^-$	$5.6^{+0.4}_{-0.4}$	$2.9^{+0.1}_{-0.3}$	$4.3^{+0.3}_{-0.3}$	$1.0^{+1.1+0.5}_{-0.7-0.5}$	$1.2^{+0.02}_{-0.02}$	$0.83^{+0.05}_{-0.05}$	$1.1^{+0.0}_{-0.1}$	
$K^{*0}\bar{K}^0$	$34.8^{+2.4}_{-2.3}$	$17.3^{+1.2}_{-1.1}$	$26.4^{+1.8}_{-1.8}$	$23.5^{+4.6+3.1}_{-3.9-3.1}$	$7.1^{+0.4}_{-0.4}$	$5.6^{+0.2}_{-0.4}$	$6.8^{+0.4}_{-0.4}$	
$\rho^0\eta$	$16.6^{+0.9}_{-1.0}$	$8.1^{+0.5}_{-0.4}$	$12.5^{+0.7}_{-0.7}$	$10.0^{+2.2+1.0}_{-1.9-1.0}$	$3.3^{+0.2}_{-0.2}$	$2.4^{+0.2}_{-0.1}$	$3.1^{+0.2}_{-0.2}$	
$\rho^0\eta'$	$8.6^{+0.6}_{-0.5}$	$4.3^{+0.3}_{-0.4}$	$6.6^{+0.4}_{-0.4}$	$2.1^{+4.7+0.2}_{-1.6-0.2}$	$2.1^{+0.1}_{-0.1}$	$1.5^{+0.1}_{-0.0}$	$2.0^{+0.1}_{-0.1}$	
$\omega\eta$	$1.5^{+0.1}_{-0.1}$	$0.76^{+0.03}_{-0.07}$	$1.1^{+0.1}_{-0.1}$	$2.3^{+1.8+0.5}_{-1.0-0.5}$	$0.31^{+0.02}_{-0.02}$	$0.22^{+0.02}_{-0.01}$	$0.29^{+0.02}_{-0.01}$	
$\omega\eta'$	$0.79^{+0.06}_{-0.06}$	$0.39^{+0.03}_{-0.03}$	$0.60^{+0.04}_{-0.04}$	<17.1	$0.20^{+0.01}_{-0.02}$	$0.14^{+0.01}_{-0.01}$	$0.18^{+0.012}_{-0.01}$	
$\phi\eta$	$19.1^{+1.1}_{-1.1}$	$9.6^{+0.6}_{-0.6}$	$14.6^{+0.8}_{-0.9}$	$2.1^{+1.9+0.2}_{-1.2-0.2}$	$4.3^{+0.2}_{-0.2}$	$3.3^{+0.2}_{-0.2}$	$4.1^{+0.1}_{-0.2}$	$2.9^{+0.5+0.1}_{-0.5-0.1}$
$\phi\eta'$	$22.6^{+1.4}_{-1.3}$	$11.5^{+0.8}_{-0.7}$	$17.4^{+1.1}_{-1.0}$	<12.6	$5.8^{+0.3}_{-0.3}$	$4.4^{+0.2}_{-0.3}$	$5.4^{+0.4}_{-0.3}$	

From Eqs. (55) and (56), we can see that, if neglecting the fragmentation contribution $F_{g,h}$, the cross sections for production of $\rho^+\pi^-$ and $\rho^0\pi^0$ in e^+e^- annihilation should be the same. At $\sqrt{s} = 3.67$ GeV, the fragmentation cannot give a large contribution as the on-shellness enhancement is not strong. Thus theoretical calculation predicts that the ratio $R_1 = \frac{\sigma(e^+e^-\to\rho^+\pi^-)}{\sigma(e^+e^-\to\rho^0\pi^0)}$ should be around 1. From Table II, one can see that this prediction is consistent with the CLEO-c results. At higher energies, the enhancement effect becomes more important. This effect can weaken $e^+e^- \to \rho^0\pi^0$ by about ten percent at $\sqrt{s} = 10.58$ GeV, relative to $e^+e^- \to \rho^+\pi^-$. If the center mass energy is large enough, the contribution from diagrams in Fig. 4 will be dominant over the other contributions.

The process $e^+e^- \to K^*K$ has previously been calculated in the PQCD (k_T factorization) and has been shown to give the correct order of magnitude for the form factors [29]. But they assume SU(3) symmetry using asymptotic wave functions. In order to show the SU(3) symmetry breaking effect in $e^+e^- \to K^*K$, we define the ratio:

$$R_2 = \frac{\sigma(e^+e^- \to K^{*0}\bar{K}^0)}{\sigma(e^+e^- \to K^{*+}K^-)} = \left|\frac{1 + \frac{F_c+F_d}{F_a+F_b}}{2 - \frac{F_c+F_d}{F_a+F_b}}\right|^2. \quad (69)$$

If we assume that SU(3) symmetry works well, then the light-cone distribution amplitude of K and K^* is completely symmetric under the exchange of the momentum fractions of quark and antiquark. We will have $F_a + F_b = F_c + F_d$, then $R_2 = 4$ can be derived directly from Eqs. (59) and (60). One of the SU(3) symmetry breaking effects is that the s quark is heavier than the $n(= u, d)$ quark and carries more momentum in the final state light $K^{(*)}$ meson. The gluon which generates $\bar{s}s$ is harder than the $\bar{n}n$ generator, then the former coupling constant is smaller due to the more off-shell gluon. Consequently, this leads to a smaller contribution to the form factor $|F_a + F_b|$ than $|F_c + F_d|$. Therefore R_2 is larger than 4. Using the cross sections listed in Table II, we obtain our result for R_2:

$$R_2 = 6.0, \quad (70)$$

where only the central value is given. The CLEO-c results indicate that there is a large deviation from the SU(3) limit [8]:

$$R_2 = 23.5^{+17.1}_{-26.1} \pm 12.2. \quad (71)$$

The central value of the experimental results for R_2 seems too large, but as the uncertainties are also large, our result could be consistent with results from the CLEO-c collaboration.

For the processes involving $\eta^{(\prime)}$ such as the process $e^+e^- \to \phi\eta$, we find that the gluonic contribution is around 1% to the total cross section at $\sqrt{s} = 10.58$ GeV. This conclusion is consistent with the study on the $B \to \eta^{(\prime)}$ form factor [18]. The cross sections of $e^+e^- \to \rho(\omega)\eta^{(\prime)}$ and $\omega\pi^0$ at $\sqrt{s} = 3.67$ GeV calculated in k_T factorization are consistent with the experimental values. The result for $e^+e^- \to \phi\eta$ at $\sqrt{s} = 10.58$ GeV is also consistent with the experimental data. This indicates that k_T factorization is an effective method to deal with the infrared divergences in exclusive processes.

The measurement of cross sections at different center mass energy $\sqrt{s}$ can shed light on the s dependence. This dependence is expected as $1/s^3$ [30] or $1/s^4$ [1,31]. Our results displayed in Table II at two different scales $\sqrt{s} =$ 10.58 GeV and 3.67 GeV seem to favor the $1/s^3$ scaling. It should be noticed that we neglected the $Q = \sqrt{s}$ dependence of the light-cone wave function and next-to-leading order contributions in our calculation. Therefore the s dependence study of the cross sections is not a complete one.

As the quark or the gluon could be on-shell, we expect the amplitudes receive an imaginary part which is similar with the exclusive B decays [5,32]. The imaginary part in $e^+e^- \to \phi\eta$ at $\sqrt{s} = 10.58$ GeV is about twice as large as the real part in magnitude and a large strong phase is consequently generated. The contributions from Fig. 3 are small; contributions from Fig. 4 are small and real; the four diagrams in Fig. 2 give comparable contributions which are the main origin of the imaginary part. Unlike the B decays, a strong phase here does not make any physical meaning, since there is no electroweak phase for interference.

From Table II, we can see that, at $\sqrt{s} = 10.58$ GeV, the cross sections for many processes, especially $e^+e^- \to K^{0*}\bar{K}^0$ and $e^+e^- \to \phi\eta'$, are large enough to be detected. We suggest the experimentalists measure these channels.

In the above, we only concentrate on the exclusive production of a vector and a pseudoscalar. Applications to PP and VV productions are straightforward. The diagrams in Fig. 2 will give dominant contributions, where the final state must have negative charge conjugation quantum number $C = -1$. Then only three channels for PP are allowed through one photon annihilation: $e^+e^- \to \pi^+\pi^-$, $e^+e^- \to K^+K^-$, and $e^+e^- \to K^0\bar{K}^0$. If U-spin is well respected, d and s quarks are symmetric in K^0 and the cross section of $e^+e^- \to K^0\bar{K}^0$ is zero. The nonzero result for $e^+e^- \to K^0\bar{K}^0$ can reflect the size of U-spin symmetry breaking. For production of VV, the analysis is similar. Two flavor-singlet vector mesons cannot be produced through one photon annihilation diagram either, but these productions could receive large additional contributions [25].

B. Theoretical uncertainties

One of the major uncertainties in our computations comes from the distribution amplitudes for the pseudoscalar and vector mesons. The dependence on the longitudinal distribution amplitudes has been studied intensively in the exclusive B decays [33]. They will give 10%–20% uncertainties here too. In the following, we will focus on the transverse momentum distribution. In the PQCD approach, the intrinsic transverse momentum is taken into account. The resummation of large double logarithms results in the Sudakov factor which suppresses the large b region's contribution. As we can see from Eq. (28), the transverse momentum distribution function also suppresses the contribution from the large b region. For momentum transfer of a few GeV, the transverse momentum distribution function damps more than the Sudakov factor [23]. This suppression makes the PQCD approach more self-consistent. So we expect that there is an obvious suppression for the production rate of $e^+e^- \to VP$ at $\sqrt{s} = 3.67$ GeV if the transverse momentum distribution amplitude is taken into account. However, at present, it is still a lack of first-principle study on the intrinsic transverse momentum distribution. The simple form is chosen as the Gaussian form discussed in Eq. (28) or the following one,

$$\Sigma(x, b) = \exp\left[-\frac{x(1-x)b^2}{4a^2}\right], \tag{72}$$

where a is the transverse size parameter as β. As a simple test, we can choose $a = 1$ which is consistent with the value used in [33]. Comparing with the form in Eq. (28), we can see that at $x = 1/2$, the two different forms coincide. For small or large x, the second form cannot give the same strong suppression as the first form [Eq. (28)]. We can expect the suppression of the results of taking the second form is less effective than the first one. In Table II, we give three different kinds of results: without the intrinsic momentum distribution (denoted as $S1$), i.e. $\Sigma = 1$; with the first distribution as Eq. (28) (denoted as $S2$); with the second kind as Eq. (72) (denoted as $S3$). Comparing the different results in Table II, we find that at small center mass energy $\sqrt{s} = 3.67$ GeV the suppression from transverse momentum distribution is more effective: the suppression is 50% for $S2$ and 20% for $S3$. Since the results depend on the explicit form of transverse momentum distribution, more experimental results are needed.

In this calculation, we only present the leading order calculations. The complete next-to-leading order calculations are much more complicated [34]. For a simple estimate of the size of the next-to-leading order contribution, we use the traditional method varying $\Lambda_{\rm QCD}$ and the factorization scale t in Eqs. (39), (49), and (53): $\Lambda_{\rm QCD} = (0.25 \pm 0.05)$ GeV; changing the hard scale t from $0.75t$ to $1.25t$ (not changing $1/b_i$). We find that our results are not sensitive to these changes. This implies that the next-to-leading order contribution is probably not very large.

IV. CONCLUSIONS

In this paper, we have studied the exclusive processes $e^+e^- \to VP$ in the PQCD approach based on the k_T factorization. We give three different kinds of results corresponding to different transverse momentum distribution functions. With the proper distribution function, our results can be consistent with the experimental results. The two different transverse momentum distribution functions $S2$ and $S3$ can give about 50% and 20% suppression, respectively, at center mass energy $\sqrt{s} = 3.67$ GeV. We have included the gluonic contribution for the processes involving $\eta^{(\prime)}$ meson whose effect is found tiny. We have also included the contribution in which the neutral vector mesons ρ^0, ω, and ϕ are produced by an additional photon. This contribution could be neglected at center mass energy $\sqrt{s} = 3.67$ GeV, while these diagrams could induce about 10% difference between $e^+e^- \to \rho^0\pi^0$ and $e^+e^- \to \rho^+\pi^-$ at $\sqrt{s} = 10.58$ GeV. The s dependence of the cross section has been directly studied which indicates that the $1/s^3$ scaling is more favored than $1/s^4$.

ACKNOWLEDGMENTS

We would like to thank Y. Jia and Y. L. Shen for useful discussions and suggestions. This work is partly supported by National Science Foundation of China under Grants No. 10475085 and No. 10625525.

[1] G. P. Lepage and S. J. Brodsky, Phys. Rev. Lett. **43**, 545 (1979); **43**, 1625(E) (1979); Phys. Lett. **87B**, 359 (1979); Phys. Rev. D **22**, 2157 (1980); S. J. Brodsky and G. P. Lepage, Phys. Rev. D **24**, 2848 (1981).

[2] A. V. Efremov and A. V. Radyushkin, Phys. Lett. **94B**, 245 (1980); V. V. Braguta, A. K. Likhoded, and A. V. Luchinsky, Phys. Rev. D **72**, 074019 (2005); Phys. Lett. B **635**, 299 (2006).

[3] A. V. Manohar and I. W. Stewart, arXiv:hep-ph/0605001.

[4] H. N. Li and G. Sterman, Nucl. Phys. **B381**, 129 (1992).

[5] H. N. Li and H. L. Yu, Phys. Rev. Lett. **74**, 4388 (1995); Y. Y. Keum, H. N. Li, and A. I. Sanda, Phys. Lett. B **504**, 6 (2001); Phys. Rev. D **63**, 054008 (2001); C. D. Lü, K. Ukai, and M. Z. Yang, Phys. Rev. D **63**, 074009 (2001); D. S. Du, C. H. Huang, Z. T. Wei, and M. Z. Yang, Phys. Lett. B **520**, 50 (2001); C. D. Lü and M. Z. Yang, Eur. Phys. J. C **23**, 275 (2002); A. Ali *et al.*, arXiv:hep-ph/0703162.

[6] M. Ablikim, Phys. Rev. D **70**, 112007 (2004).

[7] N. E. Adam *et al.* (CLEO Collaboration), Phys. Rev. Lett. **94**, 012005 (2005).

[8] G. S. Adams *et al.* (CLEO Collaboration), Phys. Rev. D **73**, 012002 (2006).

[9] B. Aubert *et al.* (*BABAR* Collaboration), Phys. Rev. D **74**, 111103 (2006).

[10] For an explicit discussion of the similarity of e^+e^- annihilation and the annihilation diagrams in B decays, please see the talk given by A. Kagan in 4th International Workshop on the CKM Unitarity Triangle (CKM 2006), Nagoya, Japan, 2006.

[11] W.-M. Yao *et al.* (Particle Data Group), J. Phys. G **33**, 1 (2006).

[12] P. Ball and R. Zwicky, Phys. Rev. D **71**, 014029 (2005).

[13] P. Ball and R. Zwicky, J. High Energy Phys. 04 (2006) 046.

[14] V. L. Chernyak and A. R. Zhitnitsky, Phys. Rep. **112**, 173 (1984); V. M. Braun and I. E. Filyanov, Z. Phys. C **44**, 157 (1989); P. Ball, J. High Energy Phys. 09 (1998) 005; V. M. Braun and I. E. Filyanov, Z. Phys. C **48**, 239 (1990); A. R. Zhitnitsky, I. R. Zhitnitsky, and V. L. Chernyak, Yad. Fiz. **41**, 445 (1985) [Sov. J. Nucl. Phys. **41**, 284 (1995)]; P. Ball, J. High Energy Phys. 01 (1999) 010.

[15] V. M. Braun and A. Lenz, Phys. Rev. D **70**, 074020 (2004); P. Ball and A. N. Talbot, J. High Energy Phys. 06 (2005) 063; P. Ball and R. Zwicky, Phys. Lett. B **633**, 289 (2006); A. Khodjamirian, Th. Mannel, and M. Melcher, Phys. Rev. D **70**, 094002 (2004); P. Ball, V. M. Braun, and A. Lenz, J. High Energy Phys. 05 (2006) 004.

[16] A. P. Bakulev, S. V. Mikhailov, and N. G. Stefanis, Phys. Lett. B **508**, 279 (2001); **590**, 309(E) (2004); Phys. Rev. D **67**, 074012 (2003); Phys. Lett. B **578**, 91 (2004); S. i. Nam and H. C. Kim, Phys. Rev. D **74**, 076005 (2006).

[17] T. Feldmann, P. Kroll, and B. Stech, Phys. Rev. D **58**, 114006 (1998); Phys. Lett. B **449**, 339 (1999).

[18] Y. Y. Charng, T. Kurimoto, and H. N. Li, Phys. Rev. D **74**, 074024 (2006).

[19] P. Kroll and K. Passek-Kumericki, Phys. Rev. D **67**, 054017 (2003); A. Ali and A. Y. Parkhomenko, Eur. Phys. J. C **30**, 183 (2003).

[20] M. V. Terentev, Yad. Fiz. **33**, 1692 (1981) [Sov. J. Nucl. Phys. **33**, 911 (1981)]; T. Ohrndorf, Nucl. Phys. **B186**, 153 (1981); M. A. Shifman and M. I. Vysotsky, Nucl. Phys. **B186**, 475 (1981); V. N. Baier and A. G. Grozin, Nucl. Phys. **B192**, 476 (1981); M. V. Terentev, Pis'ma Zh. Eksp. Teor. Fiz. **33**, 71 (1981) [JETP Lett. **33**, 67 (1981)]; A. V. Belitsky and D. Mueller, Nucl. Phys. **B537**, 397 (1999).

[21] P. Ball, V. M. Braun, Y. Koike, and K. Tanaka, Nucl. Phys. **B529**, 323 (1998); P. Ball and V. M. Braun, Nucl. Phys. **B543**, 201 (1999).

[22] P. Ball and V. M. Braun, Phys. Rev. D **54**, 2182 (1996); P. Ball and R. Zwicky, J. High Energy Phys. 02 (2006) 034; V. M. Braun and A. Lenz, Phys. Rev. D **70**, 074020 (2004); P. Ball and M. Boglione, Phys. Rev. D **68**, 094006 (2003).

[23] R. Jakob and P. Kroll, Phys. Lett. B **315**, 463 (1993); **319**, 545(E) (1993); N. G. Stefanis, W. Schroers, and H. C. Kim, Phys. Lett. B **449**, 299 (1999).

[24] M. Beneke, J. Rohrer, and D. Yang, Phys. Rev. Lett. **96**, 141801 (2006); C. D. Lü, Y. L. Shen, and W. Wang, Chin. Phys. Lett. **23**, 2684 (2006).

[25] M. Davier, M. Peskin and A. Snyder, arXiv:hep-ph/0606155; G. T. Bodwin, E. Braaten, J. Lee, and C. Yu, Phys. Rev. D **74**, 074014 (2006).

[26] J. Botts and G. Sterman, Nucl. Phys. **B325**, 62 (1989); N. G. Stefanis, W. Schroers, and H. Ch. Kim, Eur. Phys. J. C **18**, 137 (2000).

[27] G. Sterman, Phys. Lett. B **179**, 281 (1986); Nucl. Phys. **B281**, 310 (1987); S. Catani and L. Trentadue, Nucl. Phys. **B327**, 323 (1989); **B353**, 183 (1991); H. N. Li, Phys. Lett. B **454**, 328 (1999); Chin. J. Phys. (Taipei) **37**, 569 (1999).

[28] H. N. Li, Phys. Rev. D **66**, 094010 (2002).

[29] A. Kagan, in the 3rd International Workshop on the CKM Unitarity Triangle (CKM 2005), San Diego, USA, 2005.

[30] J. M. Gérard and G. López Castro, Phys. Lett. B **425**, 365 (1998).

[31] V. L. Chernyak and A. R. Zhitnitsky, Ref. [14]; V. L. Chernyak, arXiv:hep-ph/9906387.

[32] Y. Y. Keum and H. n. Li, Phys. Rev. D **63**, 074006 (2001).

[33] T. Kurimoto, Phys. Rev. D **74**, 014027 (2006).

[34] The $O(\alpha_s)$ corrections are being studied by S. Nandi and H. N. Li.